Enhancing the mechanical properties of BN nanosheet-polymer composites by uniaxial drawing

Rahim Jan,[1,2] Peter May,[2] Alan Bell,[3] Amir Habib,[1] Umar Kahn[2] and Jonathan N Coleman*[2]

[1]*School of Chemical and Materials Engineering, National University of Sciences and Technology, H-12 Campus, Islamabad, Pakistan*

[2]*School of Physics, CRANN and AMBER, Trinity College Dublin, Dublin 2, Ireland*

[3]*Advanced Microscopy Laboratory, CRANN, Trinity College Dublin, Dublin 2, Ireland.*

*colemaj@tcd.ie

ABSTRACT: We have used liquid exfoliation of hexagonal Boron-Nitride (BN) to prepare composites of BN nanosheets of three different sizes in polyvinylchloride matrices. These composites show low levels of reinforcement, consistent with poor alignment of the nanosheets as-described by a modified version of Halpin-Tsai theory. However, drawing of the composites to 300% strain results in a considerable increase in mechanical properties with the maximum composite modulus and strength both ~×3 higher than that of the pristine polymer. In addition, the rate of increase of modulus with BN volume fraction was up to 3-fold larger than for the unstrained composites. This is higher than can be explained by drawing-induced alignment using Halpin-Tsai theory. However, the data was consistent with a combination of alignment and strain-induced de-aggregation of BN multilayers.

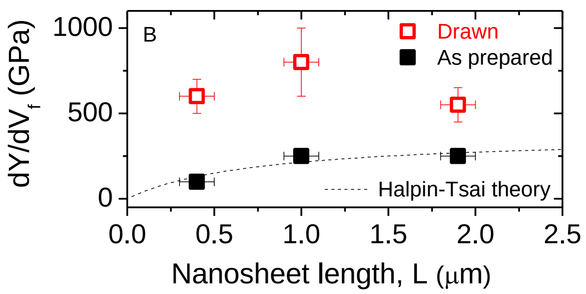

ToC fig

Uniaxial drawing of polymer-BN composites aligns the flakes, resulting in three-fold increases in stiffness and strength.

Introduction

The last few years have seen a resurgence in the study of polymers reinforced by 2-dimensional fillers. While clays have long been used to reinforce polymers,[1,2] graphene has recently surfaced as an extremely promising filler material,[3-5] due to its extremely high modulus (Y≈1 TPa) and strength (σ_B≈130 GPa).[6] Critically, it has been shown that graphene is capable of providing reinforcement at close to the theoretical maximum.[7] More recently, attention has turned to other inorganic nano-fillers such as BN, MoS_2 and WS_2, many of which occur in all dimensionalities i.e. 2D, 1D and 0D.[8,9] Such nano-materials (whether in 2D, 1D or 0D forms) have previously been used as fillers for composites, achieving improvements in a wide range of areas from thermal to tribological or adhesive properties.[10-15] Importantly, the 2D forms of many of these materials have impressive mechanical properties,[16-18] suggesting them to be ideal as reinforcing fillers in polymer-based composites. Recently, it has become possible to mix these materials with polymers because of developments which allow large scale production of 2D nanosheets in liquids.[19-24] In particular, hexagonal boron nitride (BN) nanosheets (BNNSs) are thought to have mechanical properties similar to graphene,[25] and so are of considerable interest as fillers for reinforcing plastics.[22,26,27] Of particular interest is the fact that BN nanosheets are electrically insulating allowing them to be used to improve the mechanical or barrier properties of polymers without modifying the electrical properties.

However, to our knowledge, BNNSs have demonstrated significant reinforcement (>25% increase in tensile modulus) in only two matrices: polyvinyl alcohol (PVA)[27] and polybenzimidazole.[26] Other matrixes such as epoxy, polymethylmethacrylate and polycarbonate have been studied but have shown somewhat lower levels of reinforcement.[22,28,29] It is entirely possible that the interfacial interaction between BN and these polymers is such that stress transfer is poor, rendering reinforcement ineffective. Alternatively, it may be that the low observed reinforcement is associated with other effects such as aggregation or nanosheet orientation. This would be more interesting as such problems can potentially be eradicated through improvements in processing or post-treatments.

Specifically, we could imagine addressing both of these issues through the post-treatment technique of drawing. This technique is commonly used during polymer-fiber production and involves the stretching the fibers to strains of 200-500%, depending on the polymer. This aligns the chains, increasing crystallinity and significantly improving the mechanical properties. This technique has been widely applied to composite fibers where, in addition to chain alignment, it tends to align the fillers in the direction of draw.[30-34] For a polymer reinforced with rod-like fillers, which are initially randomly orientated but become fully aligned in one direction by drawing, both strength and modulus can be increased by a factor of 8/3.[35,36] This approach has also been applied to composites with 2D fillers, although fewer papers are available, all describing clay-filled composites.[37-40] Nevertheless, these papers describe considerable increases in mechanical properties on drawing. Surprisingly, we have found no reports of drawing of composites containing graphene or BN nanosheets. In addition to inducing alignment, drawing may improve the aggregation state of the nanosheets. Strain induced delamination or deaggregation has been observed for polymer-clay composites.[41] If this could be achieved during drawing of BN filled composites, it could be used to break up small aggregates or more completely exfoliate nanosheets - further improving the mechanical properties.

We believe it is worthwhile to examine the effects of drawing in composites filled with graphene or BN nanosheets. Using BN as the filler material has the added advantage that it will allow us to explore the possibilities of improving the reinforcement in matrices where results have previously been poor. In this work we have prepared composites of polyvinylchloride (PVC) filled with BN nanosheets. We find low levels of reinforcement in the as-produced composites which we attribute to lack of alignment of the nanosheets and possibly incomplete exfoliation of the BN. However, on drawing the composites to 300% strain we find a considerable increase in mechanical properties. This is attributed to improved alignment and possibly strain-induced exfoliation or de-aggregation.

Results and Discussion

The basis of this work is the ability to exfoliate h-BN crystallites by liquid exfoliation to give dispersions containing large quantities of nanosheets.[19,21] These dispersions are ideal for further processing and composite formation. The reinforcement of composites depends strongly on the dimensions of the filler particles, specifically the length/thickness ratio.[7,35] Liquid exfoliation techniques render selection of nanosheets by size straightforward.[42] We have used centrifugation-based size selection techniques to prepare BN dispersions with three different nanosheet sizes. While we expect the nanosheet lateral size to increase with decreasing centrifugation rate, it is necessary to perform TEM analysis to quantitatively characterise the resultant nanosheet size distributions. Shown in figure 1A-C are typical TEM images of BN nanosheets prepared using centrifugation rates of 1500, 700 and 300 rpm respectively. These images clearly show few-layer nanosheets rather than BN monolayers. Careful inspection of the flake edges[43] allows the estimation of the number of monolayers per nanosheet, N. For each sample, this showed the nanosheets to be 1-10 monolayers thick with mean values around N~4. We note that these values are very approximate due to the combined problems of subjectivity and the difficulty associated with resolving individual monolayer edges. However, this data does indicate the nanosheets to be relatively well-exfoliated. It is worth remembering that monolayers are not thought to be necessary for high degrees of exfoliation. Gong et al have shown that reinforcement using graphene is maximised for N~3,[44] implying that the nanosheets used here are potentially useful fillers.

More straightforward to estimate is the mean nanosheet length, L, which we determined by measuring the lengths (i.e. the long dimension) of >120 nanosheets for each sample. These data are shown as histograms in figure 1A-C (right). We see considerable differences in the length distributions with the mean nanosheet length progressing from 0.4 to 1.0 to 1.9 μm as the rotation rate was decreased from 1500 to 700 to 300 rpm.

Using polyvinylchloride (PVC) as a matrix and the BN dispersions described above, we have prepared solution-processed composites filled with BN nanosheets of three different sizes (L=0.4, 1.0 & 1.9 μm). The composites were in the form of thin films with approximate dimensions 4cm×4cm×50μm. These films were cut into strips for tensile testing as shown in figure 2A (NB, this photo shows strips after drawing). Mechanical reinforcement in nano-composites is very sensitive to the degree of dispersion of the nano-filler. To test this we analysed the interior of the composites via helium ion microscopy of fracture surfaces. For the as-prepared composites, fracture surfaces were prepared by freeze-fracture in liquid nitrogen while the drawn composites were fractured under tensile strain. Helium ion analysis showed no evidence of large aggregates of BN nanosheets protruding from the fracture surfaces. Example images (figure 2B-C) show either small aggregates or individual flakes protruding from the polymer. This data implies the dispersion state of the nanosheets to be very good in these composites.

The composites were characterised mechanically by tensile testing. Typical stress strain curves are shown (figure 2D) for both the as-prepared polymer and the composite prepared with the 0.11 vol% of L=1.0 μm nanosheets. It is clear from this data that adding only a very small amount of BN nanosheets results in non-trivial increases in both strength and modulus. However, the strain at break varied considerably from sample to sample with no apparent pattern. As such, we will not analyse it in this paper.

We plot the Young's moduli, Y, as derived from the stress-strain curves, as a function of BN volume fraction, V_f, in figure 3. For each nanosheet length, the modulus increases roughly linearly with volume fraction before falling off at higher volume fraction. The fall-off is usually attributed to nanosheet aggregation and has been observed before for both BN and graphene based composites.[7,27,37,45,46] We find that the maximum modulus observed in all cases was just over 1.5 GPa (figure 4A), only slightly above the value of 1.45 GPa for the as-prepared polymer. We also measured the rate of increase of modulus, dY/dV_f, as shown in figure 4B. This increased from ~100 GPa to ~250 GPa as L was increased from 0.4-1.9 μm. These values are rather low compared to values of dY/dV_f~670 GPa previously reported for BN/PVA composites (L=1.3 μm).[27]

To understand this behaviour, we analyse the data using Halpin-Tsai theory.[47] The Halpin-Tsai equations describe the composite modulus, Y, as a function of the filler volume fraction, V_f, the moduli of filler, Y_F, and matrix, Y_M, as well as the platelet aspect ratio, L/t. This particular model is appropriate when nanosheets are aligned in the plane of the composite and has been shown to describe composites of BN nanosheets in polymer matrices quite well.[27] Within this model, the composite modulus is given by[5,47]

$$Y = Y_M\left[\frac{1+2V_f\eta L/t}{1-V_f\eta}\right] \tag{1}$$

where

$$\eta = \frac{Y_F/Y_M - 1}{Y_F/Y_M + 2L/t} \tag{2}$$

As we shall see below, the assumption that the nanosheets lie in plane is probably not appropriate here. We address this by following Krenchel's approach to fiber reinforced composites: We introduce an orientation parameter, η_o, which lies in the range $0\leq\eta_o\leq1$, with η_o=0 representing the case where the fillers are aligned perpendicular to the applied load and η_o=1 representing the case where the fillers are aligned parallel to the applied load.[33,34,36]

This, coupled with the approximations[48] (appropriate to most nanocomposites) that $Y_F / Y_P >> 1$ and $V_f \eta << 1$, gives the expression

$$Y \approx \frac{\eta_o Y_F V_f}{\left[\dfrac{Y_F / Y_M}{2L/t} + 1\right]} + Y_M \tag{3}$$

This expression is of course analogous to the modified rule of mixtures,[35] with a slightly different form of length efficiency factor to that given by shear-lag theory. Differentiating then yields an expression for dY/dV_f:

$$\frac{dY}{dV_f} \approx \frac{\eta_o Y_F}{\left[\dfrac{Y_F / Y_M}{2L/t} + 1\right]} \tag{4}$$

To use equation 4, it is necessary to know approximately the value of Y_F. Boldrin et al quote a range of reported values for the tensile rigidity of BN nanosheets from 184 to 348 GPa nm.[18] Dividing by the effective thickness of a BN nanosheet (0.35 nm) gives a set of moduli in the range ~500 to ~1000 GPa. The midpoint of this range, 750 GPa is somewhat smaller than the modulus of graphene (~1000 GPa) even though we might expect these materials to have similar moduli.[6] However, Gong et al have shown that 2D fillers which consist of multi-layered nanosheets have effective moduli for reinforcement which are somewhat lower that the monolayer value.[44] Thus 750 GPa is probably a reasonable estimate for the effective modulus of few-layer exfoliated BN when reinforcing a polymer matrix.

Using the fixed values of Y_F=750 GPa[25] and Y_M=1.45 GPa we have fit equation 4 to the as-prepared composite data in figure 4B finding a good fit when η_o=0.5±0.25 and t=3±2nm (dashed line). We note that a good fit could not be obtained when fixing η_o=1 implying that the BN nanosheets in these composites are not aligned in the plain of the films. This would at least partially explain why the values of dY/dV_f found here are lower than in previous reports for BN-filled composites where the nanosheets were known to be aligned.[27] In composites with randomly aligned rod-like fillers, it is known that η_o=0.2.[36] However, due to the scope for multidirectional reinforcement by each nanosheet, we expect this number to be larger for nanosheets. Indeed, it has recently been calculated that, for composites filled with randomly orientated 2D fillers, η_o=0.38.[49] Thus, while the uncertainty in our η_o value is too large to be certain, it is likely that in these composites, the BN nanosheets are in an intermediate state between being randomly orientated and aligned in the plane of the film. In addition, we note that the value of t found is somewhat larger than (although still within error) the value of t≈1.5 nm implied by the estimate of ~4 monolayers per nanosheet on average.

Once we know that the nanosheets are not well-aligned in the plane of the film, it is clear that the composite moduli could be increased by improving alignment. This can be achieved by drawing the composites as described below (see methods). In order to draw our BN/PVC composites, we applied a uniaxial strain of 300%. The elongation was then locked in by a combination of annealing and cooling. This procedure was applied to a range of volume fractions for composites filled with BN nanosheets of all three sizes. We measured the mechanical properties by tensile testing as before. Typical stress strain curves are shown in figure 2D alongside the undrawn data. It is clear from these curves that both modulus and strength can be enhanced considerably by drawing. In addition, the stain at break was generally reduced by drawing. However this data was very scattered so we will not analyse it here.

To assess this in more detail, we plot the moduli as a function of nanosheet volume fraction for all three composite types in figure 3 alongside the undrawn data. From this data, three clear effects of drawing can be seen. The modulus of the neat polymer increases from 1.45 GPa to 2 GPa, probably due to chain alignment. More interesting is the fact that the maximum modulus observed is roughly 2.75 GPa in each case (figure 4A), considerably higher than the undrawn case. Perhaps most interesting is the fact that the rate of reinforcement (dY/dV_f, figure 4B) is considerably higher than in the undrawn case, reaching 800±200 GPa for the L=1.0 μm sample. Interestingly, the fractional increase in dY/dV_f (i.e. the ratio of dY/dV_f for drawn and undrawn samples) is considerably higher for the samples with smaller nanosheets (figure 4C). For example, drawing resulted in a 6-fold increase in dY/dV_f for the L=0.4 μm sample. However, because these smaller flakes displayed lower reinforcement to start with, the resultant dY/dV_f is lower than that observed for the L=1.0 μm sample.

The simplest explanation for these results would be that drawing resulted in the alignment of the nanosheets giving a value of η_o close to 1. However, the data does not support this explanation. We have plotted equation 4 on figure 4B, taking Y_F=750 GPa,[25] and t=3 nm as before but now using Y_M=2 GPa (as observed experimentally) and η_o=1 to simulate complete alignment (solid red line). We find that, while this line coincides with the

L=1.9 μm sample, it falls considerably below the data points for the L=0.4 and 1.0 μm samples. This means that nanosheet alignment alone cannot explain the effect of drawing on the mechanical properties of these composites. While the additional contribution to modulus for the L=0.4 and 1.0 μm samples is not understood, we describe an observation which may shed light on this issue. If we plot equation 4 on figure 4B with Y_F=750 GPa, Y_M=2 GPa and η_o=1 as before but this time with t=1.25 nm, we find a curve (red dashed line) which passes very close to the error regions of all three drawn data points. This means that the drawn data is consistent with a combination of complete alignment and a reduction of nanosheet thickness compared to the undrawn samples. We speculate that, during drawing, the complex flow fields within the composite can result in the application of local shear to nanosheets resulting in shear-delamination of the few-layer flakes and so a commensurate thickness reduction. We suggest that such shear-delamination can only occur for flakes which are initially misaligned and will not occur in an aligned composite. We note that such behaviour has previously been observed for clay-filled composites so it is not un-reasonable that it should occur here.[41]

We have also measured the composite strength as a function of BN volume fraction for as-prepared composites and composites which had been drawn to 300% as shown in figure 5. Here the behaviour is very similar to that observed for the moduli. The as-prepared composites displayed very slight increases in strength, with larger nanosheets giving marginally better performance. However, after drawing, in all cases both polymer and composite strength increased significantly. The polymer strength increased from 60 to 100 MPa, probably due to chain alignment as before. In addition, the degree of reinforcement increased significantly with the best performance displayed by the L=1.0 μm sample which displayed a maximum strength of ~160 MPa for V_f~0.12%. This compares to a maximum strength of ~80 MPa in the undrawn composites.

As observed for the modulus, the strength saturates for both drawn and undrawn composites. In the drawn samples, the strength saturated for values of V_f above 0.1-0.2 %, very similar to what was observed in the modulus data. However, for the undrawn samples, the strength saturates at values of V_f~0.02%, much lower than for the undrawn samples. These results are interesting and may correlate with the strain-induced delamination suggested above. It is known that composite strength tends to more sensitive to the degree of dispersion of the nanofiller than the modulus.[50] This is because non-uniformities, such as aggregates, tend to act as stress-concentrating centres, instigating early failure. It is possible that the first aggregates start to occur in the as-prepared composites at V_f~0.02%. These would predominately affect the strength resulting in the observed saturation. However, if drawing can exfoliate nanosheets due to local shearing as suggested above, it is likely that drawing can break up aggregates, This would remove the stress-concentration centres and allowing strength enhancement to persist to higher volume fractions.

In conclusion, we have prepared composites of PVC filled with BN nanosheets of various sizes. We find relatively low levels of reinforcement largely because of the non-aligned nature of the nanosheets. However, drawing the composites to 300% strain results in relatively large increases in both modulus and strength. These increases are too large to be explained solely by nanosheet alignment. We hypothesise that the additional reinforcement is due to strain-induced exfoliation or de-aggregation. We suggest that these methods are not just useful for BN composites but can be applied to composites filled with graphene or other 2D fillers.

Methods

As-supplied boron nitride powder (Saint Gobain h-BN, high purity, average crystallite size <50 micron) was added to 60 ml of N-methyl-pyrrolidone (NMP) at a concentration of 20 mg/ml. This mixture was sonicated for 48 hrs using a flat head probe sonic tip. This procedure is well known to yield good quality exfoliated BN nanosheets.[19] To remove any unexfoliated h-BN the dispersion was centrifuged (Hettich Mikro 22R) for 45 minutes and the supernatant, which contained the nanosheets, was collected. To control the nanosheet size, varying centrifugation rates were used (1500, 700 and 300 RPM).[42,51,52] The supernatants from all the three centrifugation rates were then filtered through PET membranes (pore size 0.4 μm). The filtered material was washed with THF and dried overnight in an oven at 60 ^{o}C. The three size-selected, dried BN powders were re-dispersed in THF by mild bath sonication (Branson 1510E-MT sonic bath) to give stock dispersions at concentrations of 2mg/ml. To assess the exfoliation state of the dispersed BN nanosheets and to measure their dimensions, a few drops of dispersion from each size-selected sample were dropped onto holey carbon grids (400 mesh) and analysed using a Jeol 2100 TEM at 200kV.

To make composites films, PVC (Sigma Aldrich) was dissolved in THF at a concentration of 100 mg/ml by overnight stirring. Various volumes of the stock dispersion (BN/THF, 2 mg/ml) were added to PVC/THF solution to make composite dispersions with a range of BN mass fractions. Each dispersion was sonicated for 4 hrs in sonic bath (Branson 1510E-MT sonic bath), followed by dropcasting into Teflon trays. In all cases, the total liquid volume and solids mass were kept constant (BN+PVC=160 mg) to avoid any drying related variation from sample to sample. Two types of composites were made from each particle size. "As prepared" composites were dried at 25 ^{o}C for 24 hrs followed by another period at 65 ^{o}C for 72 C. However, those composites which would later be drawn were dried initially at 25 ^{o}C for 24 hrs only. These samples were dried to a much lesser extent, to ensure the presence of residual trapped solvent. This solvent will act as a plasticiser allowing the samples to be drawn to large strains, without any heating of the sample. The latter set of composites were drawn to a strain of 300% at a rate 5 mm/min in Zwick tensile tester with 100 N load cell. All drawn samples were clamped to avoid any shrinkage and then dried again at 65 ^{o}C for 72 Hrs. Afterwards, they were cooled ambiently to room temperature where they were held for at least four hours before testing. No shrinkage was observed over this time period.

Helium ion microscopy was performed on film fracture surfaces with a Zeiss Orion Plus. The working distance was ~5 mm and a 20 µm aperture was used. The beam current was 0.5 pA with a tilt of 15 degrees. All samples were subsequently mechanically tested using a Zick tensile tester at a strain rate of 5 mm/min using a 100N load cell.

We acknowledge the European Research Council for financial support via the grant SEMANTICS.

Figures

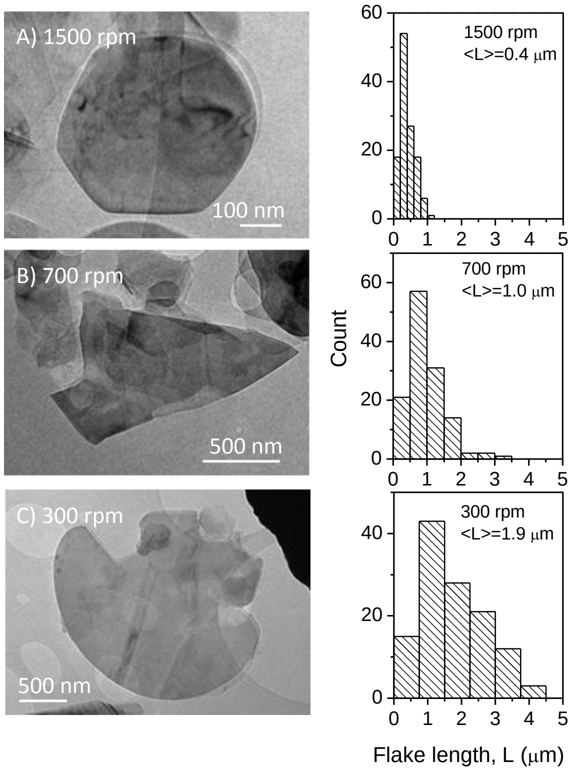

Figure 1: Transmission electron microscopy characterisation of exfoliated, size-selected BN nanosheets. On the left are sample TEM images while on the right are histograms found by measuring the lengths of ~120 nanosheets from the TEM images. Samples were prepared by centrifugation at A) 1500 rpm, B) 700 rpm and C) 300 rpm.

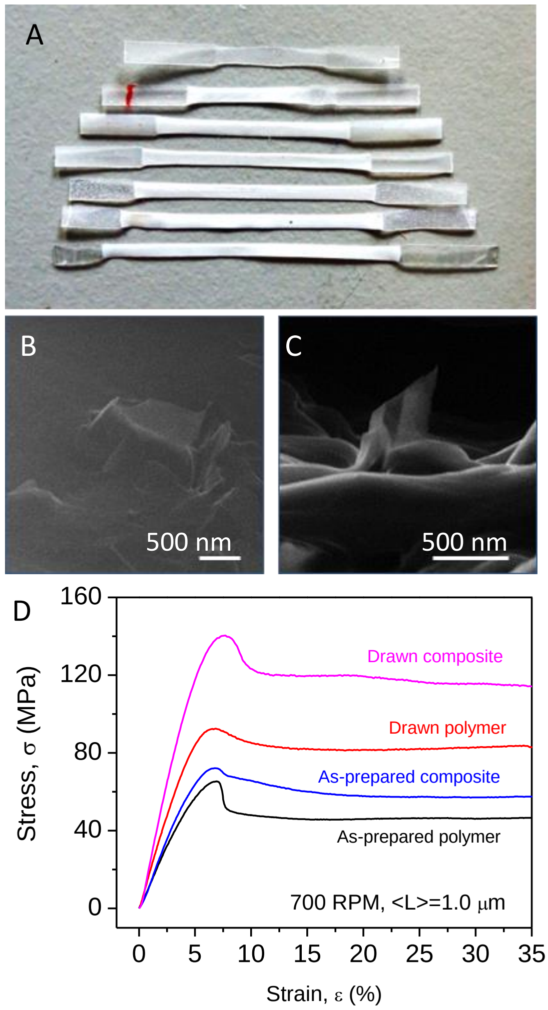

Figure 2: A) Photograph of BN-PVC films, cut into strips and drawn to various degrees. B-C) Helium ion microscope images of BN nanosheets protruding from a fracture surface of B) an as-prepared composite broken by freeze-fracture and C) a drawn composite which had subsequently been broken under tensile strain. In both B and C, the BN flakes were prepared at 700 rpm (i.e. mean length=1 micron) while the BN content was 1%. D) Representative stress strain curves showing the effects of both addition of BN and drawing on the mechanical properties of the PVC. The composites shown here were filled with 0.11 vol% BN nanosheets of mean length 1.0 μm (centrifuged at 700 rpm).

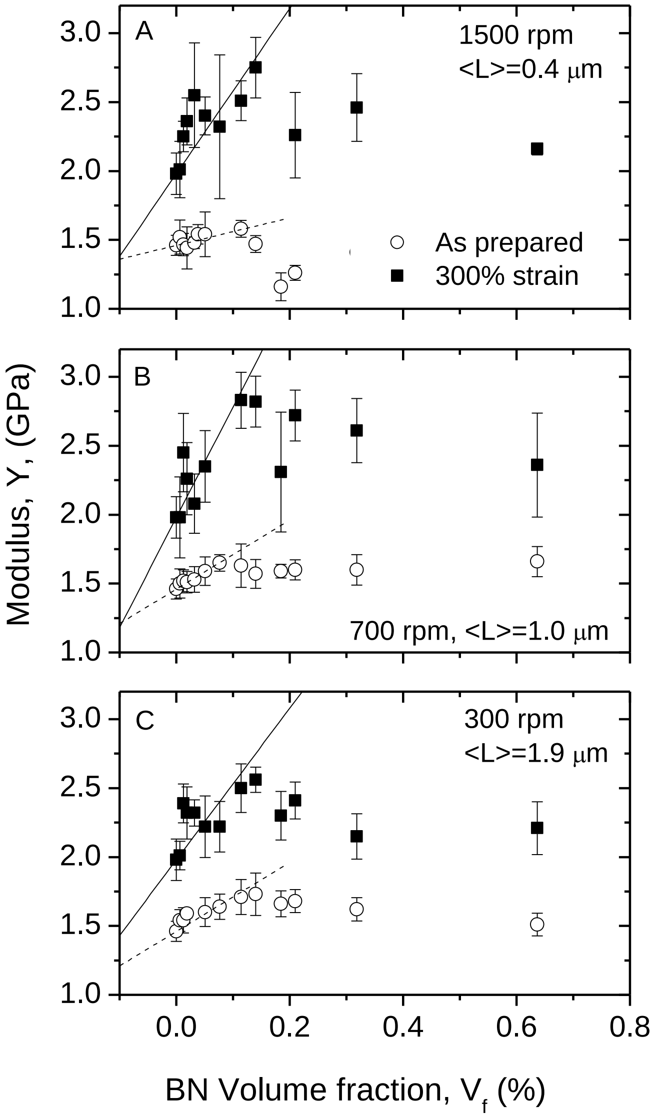

Figure 3: Young's modulus of BN nanosheet-polyvinylchloride composites plotted as a function of BN volume fraction. Data is shown for nanosheets prepared at different centrifugation rates and so with different lateral sizes: A) <L>=0.4 μm, B) <L>=1.0 μm and C) <L>=1.9 μm. In all cases, data is shown for as-prepared and drawn (300% strain) samples. The lines represent fits to the linear regions of the curves.

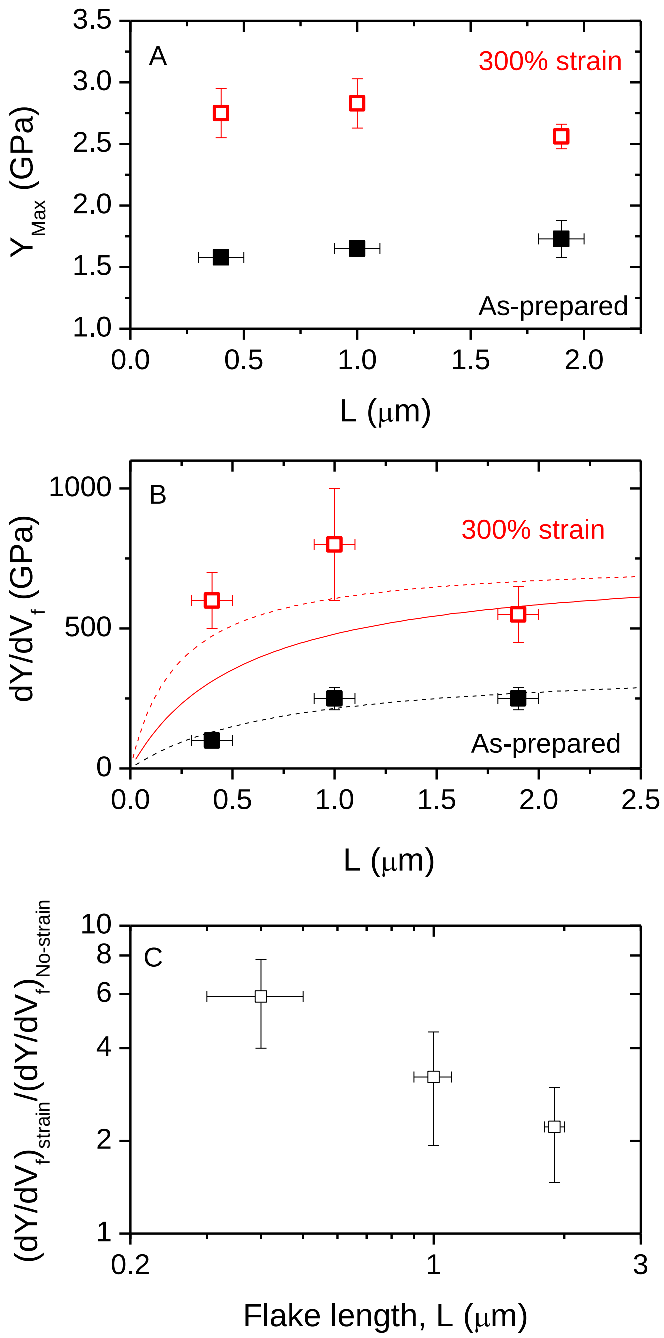

Figure 4: A) Maximum observed modulus as a function of mean nanosheet length. B) Rate of increase of modulus with BN volume fraction, dY/dV_f, for each nanosheet length with and without drawing to 300% strain. The black dashed line is a fit to equation 4 with fitting yielding η_o=0.5 and t=3 nm. The solid line is a plot of equation 4 with η_o=1 and t=3 nm while the red dashed line is a plot of equation 4 with η_o=1 and t=1.25 nm. C) Ratio of dY/dV_f after drawing to dY/dV_f in the absence of drawing, plotted versus mean nanosheet length.

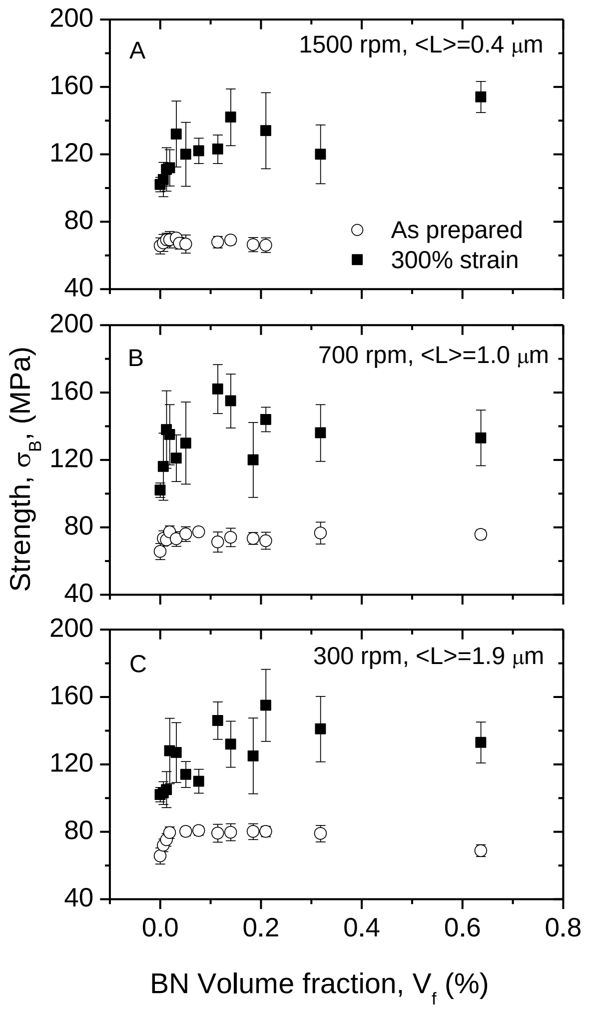

Figure 5: Ultimate tensile strength of BN nanosheet-polyvinylchloride composites plotted as a function of BN volume fraction. Data is shown for nanosheets prepared at different centrifugation rates and so with different lateral sizes: A) <L>=0.4 μm, B) <L>=1.0 μm and C) <L>=1.9 μm. In all cases, data is shown for as-prepared and drawn (300% strain) samples.

References

[1] Y. Fukushima and S. Inagaki, *Journal of Inclusion Phenomena*, **5**, 1987, 473.
[2] S. Pavlidou and C. D. Papaspyrides, *Progress in Polymer Science*, **33**, 2008, 1119.
[3] T. Kuilla, S. Bhadra, D. H. Yao, N. H. Kim, S. Bose, and J. H. Lee, *Progress in Polymer Science*, **35**, 2010, 1350.
[4] S. Stankovich, D. A. Dikin, G. H. B. Dommett, K. M. Kohlhaas, E. J. Zimney, E. A. Stach, R. D. Piner, S. T. Nguyen, and R. S. Ruoff, *Nature*, **442**, 2006, 282.
[5] R. J. Young, I. A. Kinloch, L. Gong, and K. S. Novoselov, *Composites Science and Technology*, **72**, 2012, 1459.

6 C. Lee, X. D. Wei, J. W. Kysar, and J. Hone, *Science*, **321**, 2008, 385.
7 P. May, U. Khan, A. O'Neill, and J. N. Coleman, *Journal of Materials Chemistry*, **22**, 2012, 1278.
8 D. Golberg, Y. Bando, Y. Huang, T. Terao, M. Mitome, C. C. Tang, and C. Y. Zhi, *ACS Nano*, **4**, 2010, 2979.
9 R. Tenne and M. Redlich, *Chemical Society Reviews*, **39**, 2010, 1423.
10 M. Shneider, L. Rapoport, A. Moshkovich, H. Dodiuk, S. Kenig, R. Tenne, and A. Zak, *Physica Status Solidi a-Applications and Materials Science*, **210**, 2013, 2298.
11 C. S. Reddy, A. Zak, and E. Zussman, *Journal of Materials Chemistry*, **21**, 2011, 16086.
12 M. Naffakh, A. M. Diez-Pascual, M. Remskar, and C. Marco, *Journal of Materials Chemistry*, **22**, 2012, 17002.
13 A. Fores, M. Naffakh, A. M. Diez-Pascual, F. Ania, and M. A. Gomez-Fatou, *Journal of Physical Chemistry C*, **117**, 2013, 20936.
14 H. Dodiuk, O. Kariv, S. Kenig, and R. Tenne, *Journal of Adhesion Science and Technology*, **28**, 2014, 38.
15 H. B. Cho, T. Nakayama, T. Suzuki, S. Tanaka, W. H. Jiang, H. Suematsu, and K. Niihara, *Japanese Journal of Applied Physics*, **50**, 2011.
16 C. Ataca, H. Sahin, and S. Ciraci, *Journal of Physical Chemistry C*, **116**, 2012, 8983.
17 S. Bertolazzi, J. Brivio, and A. Kis, *ACS Nano*, **5**, 2011, 9703.
18 L. Boldrin, F. Scarpa, R. Chowdhury, and S. Adhikari, *Nanotechnology*, **22**, 2011.
19 J. N. Coleman, M. Lotya, A. O'Neill, S. D. Bergin, P. J. King, U. Khan, K. Young, A. Gaucher, S. De, R. J. Smith, I. V. Shvets, S. K. Arora, G. Stanton, H. Y. Kim, K. Lee, G. T. Kim, G. S. Duesberg, T. Hallam, J. J. Boland, J. J. Wang, J. F. Donegan, J. C. Grunlan, G. Moriarty, A. Shmeliov, R. J. Nicholls, J. M. Perkins, E. M. Grieveson, K. Theuwissen, D. W. McComb, P. D. Nellist, and V. Nicolosi, *Science*, **331**, 2011, 568.
20 V. Nicolosi, M. Chhowalla, M. G. Kanatzidis, M. S. Strano, and J. N. Coleman, *Science*, **340**, 2013, 1420.
21 P. May, U. Khan, J. M. Hughes, and J. N. Coleman, *Journal of Physical Chemistry C*, **116**, 2012, 11393.
22 C. Y. Zhi, Y. Bando, C. C. Tang, H. Kuwahara, and D. Golberg, *Advanced Materials*, **21**, 2009, 2889.
23 K. G. Zhou, N. N. Mao, H. X. Wang, Y. Peng, and H. L. Zhang, *Angewandte Chemie-International Edition*, **50**, 2011, 10839.
24 R. J. Smith, P. J. King, M. Lotya, C. Wirtz, U. Khan, S. De, A. O'Neill, G. S. Duesberg, J. C. Grunlan, G. Moriarty, J. Chen, J. Z. Wang, A. I. Minett, V. Nicolosi, and J. N. Coleman, *Advanced Materials*, **23**, 2011, 3944.
25 L. Duclaux, B. Nysten, J. P. Issi, and A. W. Moore, *Physical Review B*, **46**, 1992, 3362.
26 Y. Wang, Z. X. Shi, and J. Yin, *Journal of Materials Chemistry*, **21**, 2011, 11371.
27 U. Khan, P. May, A. O'Neill, A. P. Bell, E. Boussac, A. Martin, J. Semple, and J. N. Coleman, *Nanoscale*, **5**, 2013, 581.
28 Xuebin Wang, Amir Pakdel, Chunyi Zhi, Kentaro Watanabe, Takashi Sekiguchi, Dmitri Golberg, and Yoshio Bando, *Journal of Physics-Condensed Matter*, **24**, 2012.
29 K. Wattanakul, H. Manuspiya, and N. Yanumet, *Journal of Composite Materials*, **45**, 2011, 1967.
30 R. Haggenmueller, H. H. Gommans, A. G. Rinzler, J. E. Fischer, and K. I. Winey, *Chemical Physics Letters*, **330**, 2000, 219.
31 P. Miaudet, S. Badaire, M. Maugey, A. Derre, V. Pichot, P. Launois, P. Poulin, and C. Zakri, *Nano Letters*, **5**, 2005, 2212.
32 E. T. Thostenson and T. W. Chou, *Journal of Physics D-Applied Physics*, **35**, 2002, L77.
33 F. M. Blighe, K. Young, J. J. Vilatela, A. H. Windle, I. A. Kinloch, L. B. Deng, R. J. Young, and J. N. Coleman, *Advanced Functional Materials*, **21**, 2011, 364.
34 K. Young, F. M. Blighe, J. J. Vilatela, A. H. Windle, I. A. Kinloch, L. B. Deng, R. J. Young, and J. N. Coleman, *ACS Nano*, **4**, 2010, 6989.
35 G. E. Padawer and N. Beecher, *Polymer Engineering and Science*, **10**, 1970, 185.

[36] H. Krenchal, *Fibre reinforcement;: Theoretical and practical investigations of the elasticity and strength of fibre-reinforced materials*. (Akademisk forlag 1964).
[37] T. Agag, T. Koga, and T. Takeichi, *Polymer*, **42**, 2001, 3399.
[38] J. H. Chang, S. J. Kim, Y. L. Joo, and S. Im, *Polymer*, **45**, 2004, 919.
[39] F. P. La Mantia, N. T. Dintcheva, R. Scaffaro, and R. Marino, *Macromolecular Materials and Engineering*, **293**, 2008, 83.
[40] X. Q. Zhang, M. S. Yang, Y. Zhao, S. M. Zhang, X. Dong, X. X. Liu, D. J. Wang, and D. F. Xu, *Journal of Applied Polymer Science*, **92**, 2004, 552.
[41] G. M. Kim, S. Goerlitz, and G. H. Michler, *Journal of Applied Polymer Science*, **105**, 2007, 38.
[42] U. Khan, A. O'Neill, H. Porwal, P. May, K. Nawaz, and J. N. Coleman, *Carbon*, **50**, 2012, 470.
[43] U. Khan, A. O'Neill, M. Lotya, S. De, and J. N. Coleman, *Small*, **6**, 2010, 864.
[44] L. Gong, R. J. Young, I. A. Kinloch, I. Riaz, R. Jalil, and K. S. Novoselov, *ACS Nano*, **6**, 2012, 2086.
[45] J. Longun, G. Walker, and J. O. Iroh, *Carbon*, **63**, 2013, 9.
[46] Fang Zhang, Honglei Fan, Jin Huang, Zhongmin Su, and Lihong He, *Journal of Wuhan University of Technology-Materials Science Edition*, **28**, 2013, 773.
[47] B. Harris, *Engineering Composite Materials*. (Maney Materials Science, 1999).
[48] P. May, U. Khan, and J. N. Coleman, *Applied Physics Letters*, **103**, 2013.
[49] R.J. Young and Z.L. Li (Personal communication) 2013.
[50] J. N. Coleman, U. Khan, W. J. Blau, and Y. K. Gun'ko, *Carbon*, **44**, 2006, 1624.
[51] M. Lotya, P. J. King, U. Khan, S. De, and J. N. Coleman, *ACS Nano*, **4**, 2010, 3155.
[52] A. O'Neill, U. Khan, and J. N. Coleman, *Chemistry of Materials*, **24**, 2012, 2414.